Flame Behavior under Flame-Obstacle Interaction

Baochun Fan [1], Zhanfeng Ying, Zhihua Chen , Jingfang Ye

Laboratory of Transient Physics, Nanjing Univeristy of Science & Technology,
Nanjing 210094, China

1 Introduction

The presence of repeated obstacles ahead of a propagating premixed flame can result in increased flame speeds and hence increased overpressures, which may cause considerable loss in lives and damage to property. In addition, sustained acceleration in a tube can lead to deflagration to detonation transition (DDT), which may be applied in Pulse Detonation Engines (PDE). Investigations have performed with single or repeated baffle-type[1,2] and block-type obstacles[3,4], where the effects of obstacles on the propagating flame front and overpressure resulting from the premixed turbulent flame have been discussed.

In the present work, three kinds of obstacles are used to investigate the interactions between the flame fronts and obstacles. A high speed shadowgraph system is used to visualize the flame behavior in experiments and a Large-eddy simulation of a turbulent premixed flame is used in the calculations. Sequential images are obtained experimentally and numerically which display developing processes of flame fronts under.

2 Experimental set-up

The experimental setup is shown schematically in Fig 1. The rectangular cross-section combustion chamber has the length of 320 mm in length and 58×54mm2 in inner cross-section. A pair of optical glass plates is mounted for permitting high-speed flame visualization. The ignition end (left) of the chamber is closed with a flange, while the open end (right) is sealed with a thin plastic membrane. The obstacle is placed with 180mm distance from the left end of the chamber to the backward-facing surface of the obstacle. The mixture in the combustion chamber is ignited by an electric spark installed at the ignition end. A high-speed shadowgraph imaging system is used to visualize the flame propagations, which is consisted of a light source, a concave mirror and a high speed multi-lens camera.

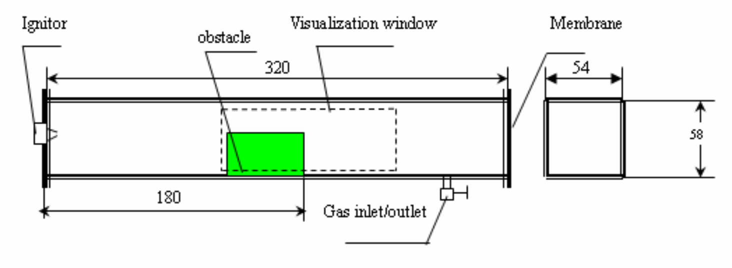

Fig.1. Schematic of the combustion vessel with an obstacle mounted.

Correspondence to : bcfan@mail.njust.edu.cn

Three kinds of obstacle are shown in Fig2. The first one (model A) is a square obstacle, the second one (model B) is a wedge obstacle, and the third one (model C) is a square obstacle with a square hole.

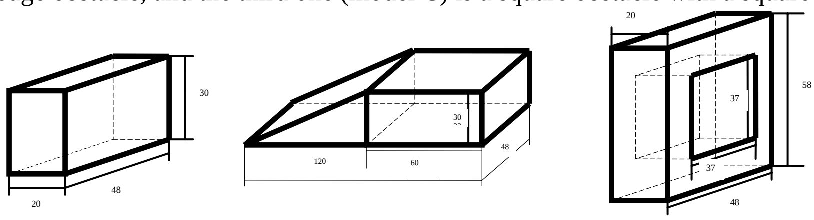

a) b) c)

Fig.2 Three kinds of obstacles

3. Mathematical Mode

The Favre filtered equations for compressible flow with combustion are written

$$\frac{\partial \rho}{\partial t} + \frac{\partial}{\partial x_j}(\rho u_j) = 0$$

$$\frac{\partial \rho Y_f}{\partial t} + \frac{\partial}{\partial x_j}(\rho u_j Y_f) = \frac{\partial}{\partial x_j} D_{eff}\, \rho \frac{\partial Y_f}{\partial x_j} - \dot{\omega}_f$$

$$\frac{\partial \rho u_i}{\partial t} + \frac{\partial}{\partial x_j}(\rho u_j u_i) = -\frac{\partial p}{\partial x_i} + \frac{\partial}{\partial x_j}\sigma_{ij}$$

$$\frac{\partial \rho E}{\partial t} + \frac{\partial}{\partial x_j}(\rho u_j E + p u_j) = \frac{\partial}{\partial x_j} q_j + \frac{\partial}{\partial x_j}(u_i \sigma_{ij}) + Q_f\, \dot{\omega}_f$$

Here $\dot{\omega}$ is reaction rate of fuel. According to the Eddy-Break-up closure(EBU)

$$\dot{\omega} = -A\rho \frac{1}{\tau_{EBU}} Y_{\lim}$$

where

$$\tau_{EBU} = C_1 \frac{\rho l_m^2}{\mu_{sgs}}$$

where l_m is the turbulent mixing length. After applying the triplet map to the inverse block size l [5] , the block-size probability density function $f(l)$ is taken to be

$$f(l) = \frac{5}{3} \frac{l^{-\frac{8}{3}}}{(L_k^{-\frac{5}{3}} - L^{-\frac{5}{3}})}$$

where L is the integral scale and L_k is the Kolmogorov scale.
Therefore

$$l_m = \frac{\int_{L_k}^{L} l\ f(l) dl}{\int_{L_k}^{L} f(l) dl}$$

The effective viscosity is modeled using constant coefficient Smagorinsky SGS model.

4. Results and Discussion

Sequences of high-speed shadowgraphs of flame front passing through model A obstacle are presented in Fig3i), and meanwhile calculated results are shown in Fig3ii) .

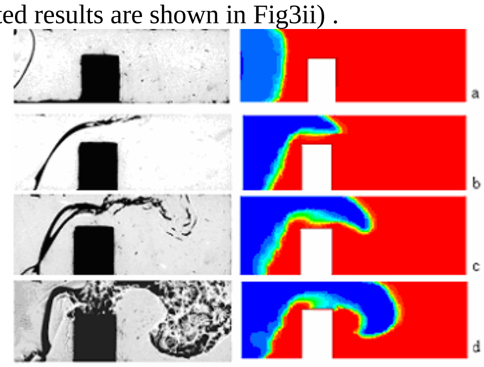

i) measured ii) calculated

Fig.3 flame front passing through model A obstacle

A smooth flame front is propagating from left to right at the beginning of passing over the obstacle (Fig3 a). When the flame passes through the narrow channel between the top surface of obstacle and the upper wall of the chamber, the flame front turbulence appears on the leading and lower parts of the flame front (Fig.3b). Then, the intensity of turbulence increases very rapidly (Fig.3c-d). The flame is drawn in by a large vortex behind the obstacle, and the leading flame is overturned towards the back and spreads quickly in all directions to form a fire ball. The flame front has been attached to the top surface of the obstacle

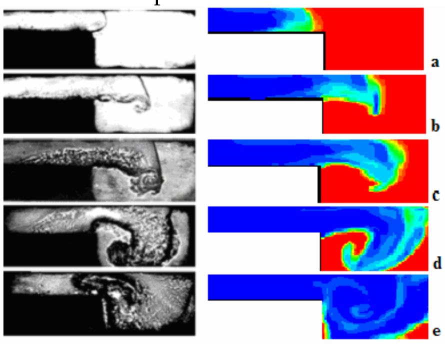

i) measured ii) calculated

Fig.4 flame front passing through model B obstacle

Another obstacle B is used, where the channel between the obstacle and the upper wall of the chamber is longer and more narrow than that for model A. Fig. 4 presents the typical series of shadow photographs and the calculated results.

As shown in Fig.4a, an accelerating smooth flame front just exits from the channel, and only a few of traces of turbulence appears near the top surface of the obstacle . It would be observed from Fig. 4b that the vortical structures appear on the lower part of flame front parallel to the bottom surface of the chamber. Then, these vortices break up into small cells which in turn make turbulence perceivable in Fig. 4c. The leading flame front is rolled up under the actionof the the vortex shown in Fig. 4d. The flame front folded on itself penetrates into the narrow channel finally as shown in Fig. 4e.

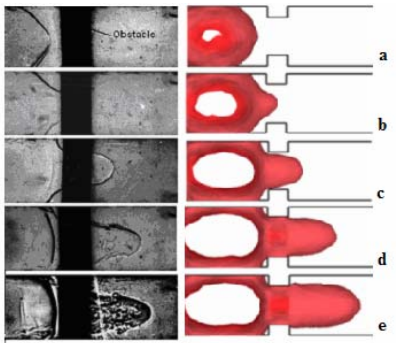

i) measured ii) calculated

Fig.5 flame front passing through model C obstacle

It emerges clearly that the turbulence-induced mechanism corresponding to the top surface of the obstacle is dominant. In order to observe the combustion behavior of the flame front facing the bottom surface of the combustion chamber, obstacle C is used. The typical series of shadow photographs and the calculated results are shown in Fig 5. The perceptible turbulence does not appear even after the flame passes through the square hole of the obstacle (Fig. 5c). The leading flame front begins to be rolled up to form vortex ring and a few traces of turbulence appear on the flame surface shown in Fig. 5d. Then, the intensity of turbulence grows up quickly, the flame brush is seen to cover all combustion region as shown in Fig. 5e. In addition, the flame fronts retarded by the obstacle in its upstream has become almost perpendicular with the walls of the combustion chamber gradually, these flame fronts become evident in subsequent images Fig. 5c-e.

Acknowledgements

The Support of this work by the China NKBRSF Project (No.2001CB409600) and the Specialized Research Fund for the Doctoral Program (SRFDP) of Higher Education (No.20050288028) is gratefully acknowledged.

References

[1] Ciccarelli G, Fowler CJ and Bardon M (2005) Effect of obstacle size and spacing on the initial stage of flame acceleration in a rough tube. Shock Waves, 14(3):161-166.

[2] Oh K-H, Kim H, Kim J-B, Lee S–E (2001) A study on the obstacle-induced variation of the gas explosion characteristics, Journal of Loss Prevention in the Process Industries, 14: 97–602.

[3] Kirkpatrick MP, Armfield SM, Masri AR and Ibrhim SS (2003) Large eddy simulation of a propagating turbulent premixed flame, Flow, Turbulence and Combustion 70:1-19

[4] Ibrahim SS, Hargrave GK and Williams TC (2001) Experimental investigation of flame/solid interactions in turbulent premixed combustion. Experimental Thermal and Fluid Science, 24:99-106.

[5] Kerstein AR(1990) Liner-eddy modeling of turbulent transport. Part 3. Mixing and diferential molecular diffusion in round jets. J.Fluid.Mech.216:411-435